

# Dispersion analysis of asymmetric band shapes: Application to the IR absorption spectrum of silica glass

A. M. EFIMOV

Vavilov State Optical Institute, 193171 St. Petersburg, Russia

H. HOBERT

Institute für Physikalische Chemie, Friedrich-Schiller Universität, Jena D-07743, Jena, Germany

E-mail: efimov@ae4050.spb.edu

The IR absorption spectrum of silica glass in the 3800 to 8000  $\text{cm}^{-1}$  region is analyzed based on the assumption of asymmetric band shapes. For simulating the asymmetric band shapes, a generalized version of the convolution model for the complex dielectric constant is proposed that involves different magnitudes of the standard deviation for an oscillator distribution in the wavenumber regions below and above the distribution center. A computational program for the dispersion analysis of the absorption spectra using such a model is developed. Best fit to the IR spectrum of silica glass obtained with the asymmetric band shapes contains no systematic errors throughout the contours of the 4400–4600 and 7000–7300  $\text{cm}^{-1}$  absorption maxima, thus having appreciably better quality than fits obtainable with the symmetric band shapes inherent in the usual convolution model. A high accuracy of simulating the 7000–7300  $\text{cm}^{-1}$  absorption maximum with the asymmetric band shapes is attained when using as few as two bands in this region, which is in contrast to available literature sources assuming four bands. The band frequencies and intensities calculated with the asymmetric and symmetric band shapes are compared.

© 2004 Kluwer Academic Publishers

## 1. Introduction

Silica glass is a widely used material, which is why the modelling of various processes of heat treatment of this glass is of importance for glass industry. For such modelling, the knowledge of the heat transfer in the glass is necessary. However, silica glass is manufactured by a variety of processes, each process generating different concentrations of water-related species in the glass. These species greatly affect the radiation conductivity that substantially determines the heat transfer in glasses and is known [1] to have a maximum in the near- and mid-IR. Therefore, the absorption of silica glass in the 3300 to 10000  $\text{cm}^{-1}$  (3 to 1  $\mu\text{m}$ ) region was studied extensively [2–5] (this absorption being mostly due to the water-related species such as the bound hydroxyl groups and interstitial water molecules). In these studies, special attention was paid to the deconvolution of a complicated absorption spectrum of silica glass in this region.

For deconvoluting the spectrum of a material into individual spectral components, or bands, either some standard empirical methods or a dispersion analysis method (see, for example, [6–8]) can be applied. Standard methods use the symmetric (typically, Gaussian) contours for the components. Gaussian contours were

used when deconvoluting the IR absorption spectrum of silica glass in the ranges of (i) the hydroxyl- and  $\text{H}_2\text{O}$ -related fundamentals, 3400–3720  $\text{cm}^{-1}$  [2], and (ii) multiphonon hydroxyl- and  $\text{H}_2\text{O}$ -related vibrations, 3800–10000  $\text{cm}^{-1}$  [3–5].

Stone and Walrafen [3] deconvoluted the asymmetric maximum in the 4400 to 4600  $\text{cm}^{-1}$  region into two individual Gaussian bands around 4450 and 4520  $\text{cm}^{-1}$  and assigned these bands to two combination modes involving the 1st or 4th component of the stretching (Si)O—H vibration<sup>1</sup> and the symmetric or asymmetric component of the stretching Si—O—Si vibration, respectively. These combination modes are denoted further by  $\nu'$  (Si)O—H +  $\nu_s$  Si—O—Si and  $\nu''''$  (Si)O—H +  $\nu_{as}$  Si—O—Si, respectively. Humbach *et al.* [5] considered the maximum in the 4400 to 4600  $\text{cm}^{-1}$  region to be a single band and assigned it to a combination mode involving some  $\nu$ (Si)O—H component and  $\nu_s$  Si—O—Si vibration.

<sup>1</sup> In [3], the idea of the splitting of the stretching (Si)O—H vibration into as many as four components was borrowed from Walrafen and Samanta [4] who assumed the occurrence of two kinds of so-called bidentate units, each unit being formed by two (Si)O—H groups.

An asymmetric absorption maximum in the 7000 to 7300  $\text{cm}^{-1}$  region was mostly considered in [3–5] to be the envelope of three Gaussian bands assigned to the overtones of three components of the (Si)O–H stretching vibration (for the reason assumed to be responsible for the splitting of the vibration, see Footnote 1). Stone and Walrafen [3] considered these overtones to be  $2\nu'''$  (Si)O–H,  $2\nu''$  (Si)O–H, and  $2\nu'$  (Si)O–H. As to the fourth band around 7380  $\text{cm}^{-1}$  that forms a weak shoulder at the high-wavenumber wing of the 7000–7300  $\text{cm}^{-1}$  envelope, Stone and Walrafen assigned this band to the combination mode such as  $2\nu'''$  (Si)O–H +  $\delta$  Si–O–Si ( $\delta$  indicating the bending mode). Yokomashi *et al.* [4] assigned the 7380  $\text{cm}^{-1}$  band to the overtone of the 1st component of the (Si)O–H stretching mode,  $2\nu'$  (Si)O–H.

The band shapes in the absorption spectra of glasses are by no means Gaussian [8–11]; therefore, the results of Gaussian deconvolutions of these spectra and, hence, the assignments for spectral components thus resolved are dubious. A more reliable solution of the problem of glass spectrum deconvolution can be obtained with a dispersion analysis method that is based on a particular analytical model for the complex dielectric constant of a material. Various versions of the dispersion analysis differing in the kind of the model used were developed for crystals [6, 7] and glasses [8–12]. Unlike standard deconvolution methods, dispersion analysis provides data on not only the spectral components but also (i) the optical constants of a material and (ii) physically meaningful optical microcharacteristics (such as the inherent frequencies of oscillators, oscillator strengths, phonon lifetimes, and also, for glasses, the widths of the oscillator distributions over frequency) denoted further by the collective term “band parameters”.

The dispersion analysis of glass spectra uses the convolution model for the complex dielectric constant (or dielectric function)  $\hat{\varepsilon}(\omega)$  as follows (see, for example, [8–12]):

$$\hat{\varepsilon}(\omega) = \varepsilon_{\infty} + \sum_{j=1}^J \frac{S_j}{\sqrt{2\pi}\sigma_j} \times \int_{-\infty}^{+\infty} \frac{\exp[-(x - \omega_j)^2/2\sigma_j^2]}{x^2 - \omega^2 - i\gamma_j\omega} dx \quad (1)$$

Here  $x$  is the variable oscillator frequency,  $\omega_j$  is the central frequency for the  $j$ -th oscillator distribution, and  $\sigma_j$  is the standard deviation for this distribution. The rest are parameters retaining the same meaning as in the classical model [6] widely used for the dispersion analysis of the IR spectra of crystals. Best fits to glass spectra obtainable with the dispersion analysis based on Equation 1 were shown [8–10] to be characterized by deviations from experiment less than the measurement error. The random errors in the band frequencies and intensities obtainable with the dispersion analysis of the absorption spectra were estimated [9] to be, for weak and/or greatly overlapped bands, around 0.5–0.6% and 10–12%, respectively.

When using the band shapes given by Equation 1, there is no need to assume as many as three hydroxyl-

and water-related components (as was made in [2]) in the narrow 3600–3700  $\text{cm}^{-1}$  region of the absorption spectrum of silica glass: two components are enough for satisfactorily simulating this region [11].

As seen, model (1) denoted further by the usual convolution model retains the symmetric peak contours for the imaginary part,  $\varepsilon''(\omega)$ , of the complex dielectric constant that are inherited from the classical model [6]. Nearly symmetric  $\varepsilon''(\omega)$  peak contours are characteristic also of another model used for the dispersion analysis of the IR spectra of crystals that is known as the factorized model [7]. A negligible asymmetry of the  $\varepsilon''(\omega)$  peak shape presupposed by the latter model is due to the variable damping coefficient alone. At the same time, a thorough theoretical consideration [13] indicates the IR band shapes in the spectra of disordered polymers to be substantially asymmetric. For the so-called boson peak in the low-frequency Raman and IR spectra of glasses, the asymmetric contour was shown to occur [14, 15] as well. So, the simulation of the spectra of glasses and other disordered materials with any model that presupposes the symmetric  $\varepsilon''(\omega)$  peak shapes seems to be a somewhat simplified approach. When aiming to a mere phenomenological simulation of the experimental absorption spectrum for a glass, the asymmetric band shapes can be easily approximated with some appropriate asymmetric function such as the step function, lognormal distribution function (as was the case for [14, 15]), and so on. However, the phenomenological simulation cannot provide data on the optical constants and band parameters, which is why the dispersion analysis of the spectrum is required for calculating these data. For implementing the dispersion analysis of glass spectra in terms of the band shape asymmetry, one needs an analytical model for  $\hat{\varepsilon}(\omega)$  that would allow for the asymmetric  $\varepsilon''(\omega)$  peak contours, whereas the usual convolution model (1) retains, as mentioned above, the symmetric  $\varepsilon''(\omega)$  peak contours. So, a search for the  $\hat{\varepsilon}(\omega)$  model applicable to spectra with an arbitrary degree of the  $\varepsilon''(\omega)$  peak asymmetry is of importance for further development of methods for spectral data treatment appropriate for glasses and other materials with disordered structures.

In view of visual asymmetry, the absorption maxima in the silica glass spectrum located in the 4400–4600 and 7000–7300  $\text{cm}^{-1}$  regions are appropriate examples for testing the applicability of models with the asymmetric  $\varepsilon''(\omega)$  peak contours to be developed. In the given research, we (i) proposed a reasonably simple analytical representation for the asymmetric band shapes based on a certain generalization of the usual convolution model, (ii) developed the corresponding computational procedure of the dispersion analysis, and (iii) tested this procedure with respect to the IR absorption maxima around 4500 and 7200  $\text{cm}^{-1}$  in the silica glass spectrum.

## 2. Experimental and computational

The sample investigated was prepared from a synthetic silica glass of type III,<sup>2</sup> 6.35 cm thick. The IR absorption

<sup>2</sup> In accord with notations proposed in [16], type III silica glass usually contains approx. 1000 ppm H<sub>2</sub>O (the glass being obtained by the hydrolysis of SiCl<sub>4</sub> in the H<sub>2</sub> + O<sub>2</sub> flame).

spectrum of the sample in the 3800 to 8000  $\text{cm}^{-1}$  was recorded with a FTIR spectrophotometer (Bruker IFS66) using the resolution of 4  $\text{cm}^{-1}$  and 256 scans. The signal/noise ratio at 7200  $\text{cm}^{-1}$  was 250.

Notably, the use of some arbitrarily chosen  $\hat{\varepsilon}(\omega)$  model allowing for the  $\varepsilon''(\omega)$  peak asymmetry would require an algorithm for the numerical integration that is entirely different compared to that used in the computational procedure of the dispersion analysis [8–10] involving Equation 1. The development of such a new algorithm can turn out to be a complicated task. For avoiding the necessity of developing the new algorithm for the numerical integration, a relatively simple (though somewhat formal) way that allowed for processing quantitatively the IR spectra containing the asymmetric bands was chosen as follows. The convolution integral in Equation 1 was replaced by two halves of such integrals differing in the magnitudes of the intensities,  $S_{j1}$  and  $S_{j2}$ , and standard deviations,  $\sigma_{j1}$  and  $\sigma_{j2}$ :

$$\hat{\varepsilon}(\omega) = \varepsilon_{\infty} + \frac{1}{\sqrt{2\pi}} \sum_{j=1}^J \left( \frac{S_{j1}}{2\sigma_{j1}} \int_{-\infty}^{+\infty} \frac{\exp[-(x - \omega_j)^2/2\sigma_{j1}^2]}{x^2 - \omega^2 - i\gamma_j\omega} dx + \frac{S_{j2}}{2\sigma_{j2}} \int_{-\infty}^{+\infty} \frac{\exp[-(x - \omega_j)^2/2\sigma_{j2}^2]}{x^2 - \omega^2 - i\gamma_j\omega} dx \right) \quad (2)$$

Here  $S_j$  and  $\sigma_j$  with subscript indices 1 and 2 correspond to the  $\omega \leq \omega_j$  and  $\omega \geq \omega_j$  frequency ranges, respectively. In a general case,  $S_{j1} \neq S_{j2}$  and  $\sigma_{j1} \neq \sigma_{j2}$ . For the symmetric bands (if any), these inequalities are replaced by equalities  $S_{j1} = S_{j2}$  and  $\sigma_{j1} = \sigma_{j2}$ , which reduces the corresponding members of the generalized Equation 2 to those of the initial Equation 1. In terms of Equation 2, the  $S_{j1}/S_{j2}$  and  $\sigma_{j1}/\sigma_{j2}$  ratios are measures for the absorption band asymmetry and the asymmetry of the oscillator distribution,<sup>3</sup> respectively. So, Equation 2 is a certain generalization of the convolution model (1) over the case of an arbitrary band asymmetry.

Based on Equation 2, a computational program for the dispersion analysis of the IR absorption spectra of glasses with the asymmetric band shapes was developed. When applying this program to the IR absorption spectrum of silica, the occurrence of the  $S_{j1} \neq S_{j2}$  and  $\sigma_{j1} \neq \sigma_{j2}$  inequalities was allowed for bands consisting the 4400 to 4600 and 7000 to 7450  $\text{cm}^{-1}$  envelopes whose asymmetry was seen visually. For the 3800–4400, 4550–7000, and 7450–8000  $\text{cm}^{-1}$  regions, the symmetric band shapes were shown to allow for simulating the experimental absorption spectrum quite satisfactorily, which is why the conditions  $S_{j1} = S_{j2}$  and  $\sigma_{j1} = \sigma_{j2}$  were imposed for these regions. For representing the total effect of strong fundamental IR oscillators

<sup>3</sup> The  $S_{j1}/S_{j2}$  and  $\sigma_{j1}/\sigma_{j2}$  ratios do not coincide with each other because the absorption band shapes are determined by not only the standard deviations but also the damping coefficients.

of silica glass matrix on the real part of the complex dielectric constant in the range under consideration,  $\varepsilon_{\infty}$  was assumed, as in [17], to be frequency-dependent, this  $\varepsilon_{\infty}$  being approximated by the Sellmeier-like function borrowed from [18].

In the dispersion analysis, the quality of a fit is known [8] to be estimated in terms of some error function,  $Q$ . The error function used in the given research was as follows:

$$Q(\{p_m\}_1^M) = \sqrt{\frac{1}{\omega_1 - \omega_2} \int_{\omega_1}^{\omega_2} [\alpha_{\text{mod}}(\omega, \{p_m\}_1^M) - \alpha_{\text{exp}}(\omega)]^2 d\omega} \quad (3)$$

Here  $\{p_m\}_1^M$  is the multitude of the oscillator parameters,  $\alpha_{\text{mod}}(\omega, \{p_m\}_1^M)$  and  $\alpha_{\text{exp}}(\omega)$  are the model absorptivity computed with these parameters and experimental absorptivity, respectively, and  $\omega_1$  and  $\omega_2$  are the wavenumber limits of a range under simulation.

With  $Q$  thus chosen, the highest attainable quality of best fit to a spectrum is reached when a condition is obeyed that is determined by inequality as follows:  $Q(\omega, \{p_m\}_1^M) < \Delta\alpha_{\text{exp}}(\omega)$ , where  $\Delta\alpha_{\text{exp}}(\omega)$  is the random error of experimental absorptivity.

### 3. Results

Fig. 1 shows the experimental spectrum of our silica glass sample in the 3850 to 7650  $\text{cm}^{-1}$  range. When simulating this spectrum, the contributions of (i) the high-frequency IR fundamentals of silica matrix [8] and (ii) the hydroxyl- and water-related bands known [11] to occur at wavenumbers less than 3650  $\text{cm}^{-1}$  to the absorption in this region were approximated by a single effective oscillator with inherent frequency close to that of the highest IR fundamental of  $\text{SiO}_2$  network. For representing bands at wavenumbers greater than 3650  $\text{cm}^{-1}$ , particular oscillators were used, initial magnitudes of their parameters being mostly borrowed from [11].

For bands simulating the 4400–4600 and 7000–7450  $\text{cm}^{-1}$  regions (Table I) in which visually asymmetric absorption maxima occur, the asymmetric band contours given by Equation 2 were used (these bands being represented by the 7th, 8th, 14th, 15th, and 16th oscillators). As in [11], the 4400–4600  $\text{cm}^{-1}$  envelope whose complicated structure is seen clearly was simulated with two bands. Though the shape of the 7000–7300  $\text{cm}^{-1}$  envelope is smooth, it was found impossible to reproduce this envelope with a single asymmetric contour. Therefore, for simulating the 7000–7300  $\text{cm}^{-1}$  envelope, two bands (as in [11]) were used and the expedience of using the asymmetric contours for these bands was analyzed.

For bands that form the structureless 3800–4400, 4550–7000, and 7450–8000  $\text{cm}^{-1}$  regions, the symmetric contours given by Equation 1 were found to be appropriate. In addition to oscillators from [11], it was found necessary to incorporate oscillators around 6900

TABLE I Inherent oscillator frequencies,  $\omega_j$ , and oscillator strengths,  $\Delta\varepsilon_{0j} = (S_{j1}/\omega_j^2 + S_{j2}/\omega_j^2)/2$ , found with the dispersion analysis based on Equation 2 to contribute to the absorption spectrum of silica glass sample in the 3800–8000  $\text{cm}^{-1}$  range

Oscillator no.	$\omega_j$ ( $\text{cm}^{-1}$ )	$\Delta\varepsilon_{0j}$	Notes	Oscillator no.	$\omega_j$ ( $\text{cm}^{-1}$ )	$\Delta\varepsilon_{0j}$	Notes
1	1180.4	$7.93 \times 10^{-6}$	Effective oscillator	10	4863.8	$7.47 \times 10^{-9}$	
2	3678.9	$4.95 \times 10^{-5}$		11	5275.3	$7.49 \times 10^{-9}$	
3	3812.0	$3.87 \times 10^{-7}$		12	5807.2	$6.25 \times 10^{-9}$	
4	3882.8	$5.67 \times 10^{-7}$		13	6931.5	$1.40 \times 10^{-8}$	
5	3964.0	$2.37 \times 10^{-7}$		14	7105.9	$1.37 \times 10^{-8}$	
6	4076.1	$1.54 \times 10^{-7}$		15	7229.3	$6.02 \times 10^{-8}$	
7	4450.9	$5.94 \times 10^{-7}$		16	7384.0	$5.08 \times 10^{-9}$	
8	4527.3	$2.55 \times 10^{-7}$		17	7533.2	$9.94 \times 10^{-10}$	
9	4630.0	$1.95 \times 10^{-9}$		18	82324.0	$2.17 \times 10^{-3}$	Effective oscillator

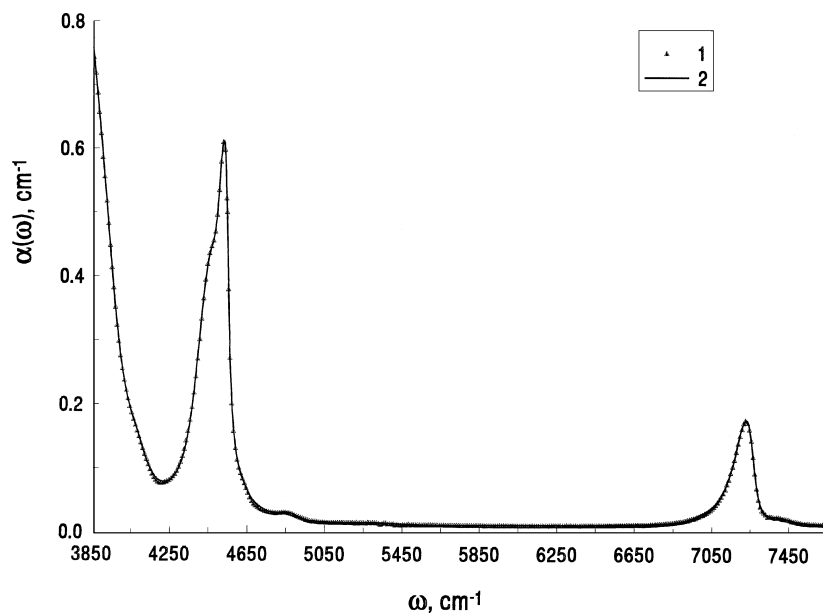


Figure 1 Overview of the IR absorption spectrum of silica glass sample in the range of the second order water-related vibrations and best fit to the spectrum obtained with the asymmetric contours given by Equation 2 for bands located in the 4400 to 4550 and 7000 to 7450  $\text{cm}^{-1}$  regions (for the rest bands, the symmetric band contours being used). (1) is experiment and (2) is best fit.

and 7500  $\text{cm}^{-1}$  and also, for approximating the contributions of the fundamental electronic excitations to the absorption in this region, another effective oscillator in the VUV. Thus, the overall number of oscillators used for simulating the spectrum under study was taken to be 18.

Table I presents the magnitudes of the band frequencies and intensities thus fitted, the intensities being expressed in terms of the oscillator strengths  $\Delta\varepsilon_{0j} = S_j/\omega_j^2$  (these quantities being the contributions of the oscillators to the static dielectric constant  $\Delta\varepsilon_0$ ). For the asymmetric band shapes given by Equation 2, the total  $\Delta\varepsilon_{0j}$  values were calculated, as averages, by  $\Delta\varepsilon_{0j} = (S_{j1}/\omega_j^2 + S_{j2}/\omega_j^2)/2$ . For comparison, the spectrum under study was fitted also with the symmetric contours given by Equation 1 for all oscillators used. Table II compares, for the 4400–4550 and 7000–7450  $\text{cm}^{-1}$  regions, the band frequencies, oscillator strengths, and standard deviations computed with the asymmetric and symmetric band contours.

Best fit to the spectrum of our silica glass sample obtained with the asymmetric band contours for

simulating the 4400 to 4550 and 7000 to 7450  $\text{cm}^{-1}$  regions is shown in Fig. 1. Fig. 2 compares, on an enlarged scale, best fits in the 4250 to 4640  $\text{cm}^{-1}$  region obtained with the asymmetric and symmetric band contours given by Equations 1 and 2, respectively. Fig. 3 shows, on an enlarged scale, best fit in the 7000 to 7450  $\text{cm}^{-1}$  region obtained with the asymmetric band contours given by Equation 2. Fig. 4 compares best fits at wavenumbers greater than 6500  $\text{cm}^{-1}$  obtained with the asymmetric and symmetric band contours given by Equations 1 and 2, respectively. Fig. 5 compares individual band shapes deconvoluted, from the 7000 to 7450  $\text{cm}^{-1}$  region, with Equations 1 and 2.

#### 4. Discussion

The inherent band frequencies computed with Equations 1 and 2 differ negligibly (Table II). The oscillator strengths vary more perceptibly, which is due to not only the greater computational errors but also differences in the spread of the total band intensity for an envelope over particular bands in the envelope depending

TABLE II Comparison of the inherent frequencies and oscillator strengths for bands in the 4400–4600 and 7000–7300  $\text{cm}^{-1}$  regions computed with the asymmetric and symmetric band shapes

Band frequency range ( $\text{cm}^{-1}$ )	Data computed with							
	Asymmetric band shapes given by Equation 2, $Q^a = 1.26 \times 10^{-3}$					Symmetric band shapes given by Equation 1, $Q^a = 2.70 \times 10^{-3}$		
	$\omega_j$ ( $\text{cm}^{-1}$ )	$\Delta\epsilon_{0j} = (S_{j1}/\omega_j^2 + S_{j2}/\omega_j^2)/2$		$\frac{S_{j1}}{S_{j2}}$	$\frac{\sigma_{j1}}{\sigma_{j2}}$	$\omega_j$ ( $\text{cm}^{-1}$ )	$\Delta\epsilon_{0j}$	
	For the bands	Total for the range				For the bands	Total for the range	
4400–4600	4450.9	$5.94 \times 10^{-7}$	$8.49 \times 10^{-7}$	1.1	4.1	4450.3	$6.27 \times 10^{-7}$	$8.56 \times 10^{-7}$
	4527.3	$2.55 \times 10^{-7}$		1.4	2.1	4523.1	$2.29 \times 10^{-7}$	
7000–7300	7105.9	$1.37 \times 10^{-8}$	$7.39 \times 10^{-8}$	2.4	2.8	7086.7	$1.38 \times 10^{-8}$	$7.28 \times 10^{-8}$
	—	—		—	—	7165.9	$1.97 \times 10^{-8}$	
7300–7600	7229.3	$6.02 \times 10^{-8}$	$6.07 \times 10^{-9}$	1.7	1.9	7231.3	$3.93 \times 10^{-8}$	$6.19 \times 10^{-9}$
	7384.0	$5.08 \times 10^{-9}$		1.3	1.3	7395.2	$4.39 \times 10^{-9}$	
	7533.2	$9.94 \times 10^{-10}$		1.0	1.0	7578.2	$1.80 \times 10^{-9}$	

<sup>a</sup>The error function  $Q$  value given by Equation 3 is determined over the entire 3800–8000  $\text{cm}^{-1}$  range.

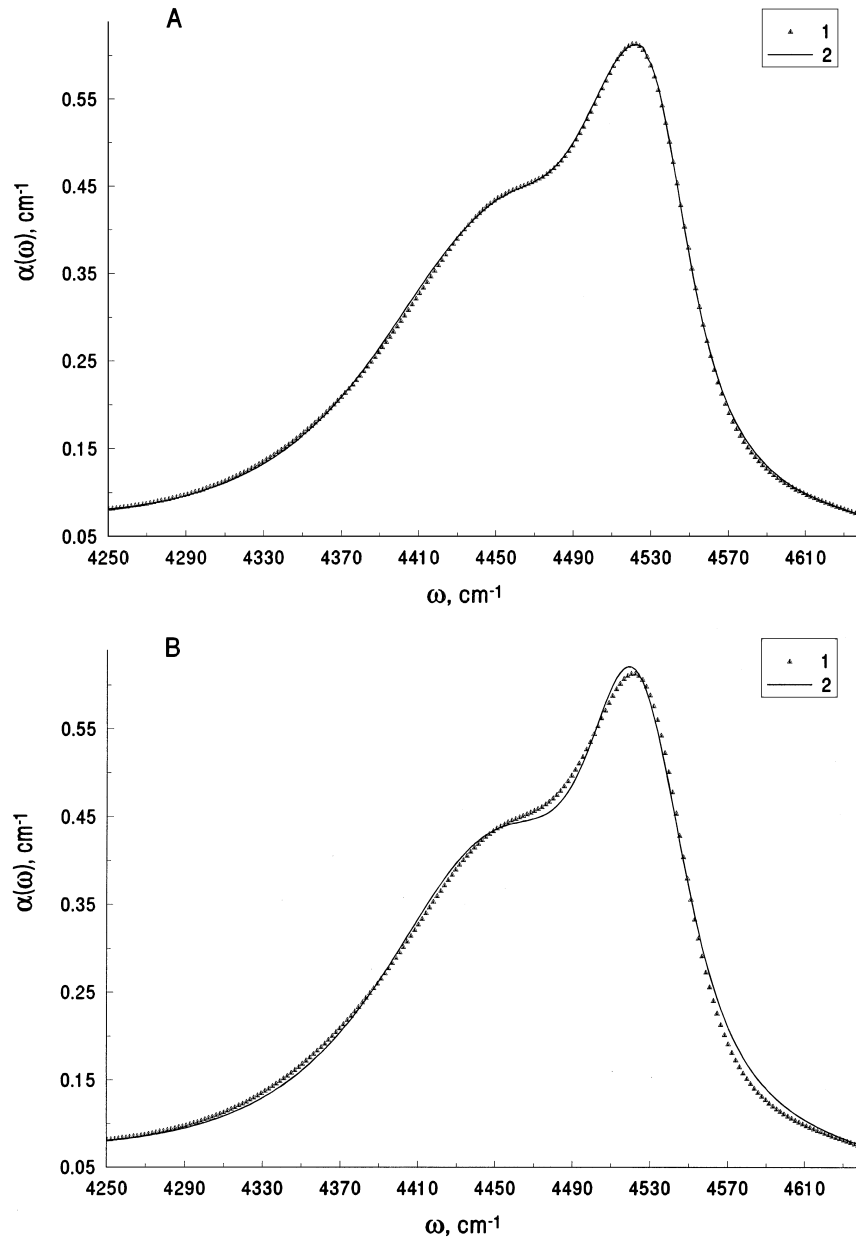


Figure 2 Best fits to the spectrum of silica glass sample in the 4250 to 4640  $\text{cm}^{-1}$  region obtained with different contours for bands around 4450 and 4525  $\text{cm}^{-1}$ . (A) Asymmetric band contours given by Equation 2. (1) is experiment and (2) is best fit. (B) Symmetric band contours given by Equation 1. (1) is experiment and (2) is best fit.

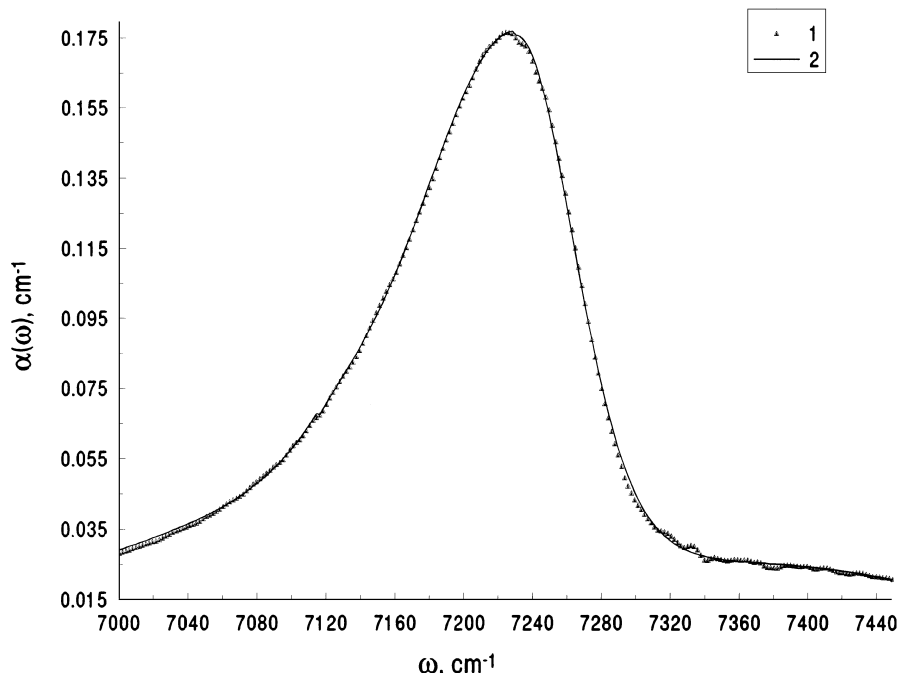


Figure 3 Best fit to the spectrum of silica glass sample in the 7000 to 7450  $\text{cm}^{-1}$  region obtained with the asymmetric band contours given by Equation 2. For simulating the 7000 to 7300  $\text{cm}^{-1}$  envelope, two bands at 7106 and 7229  $\text{cm}^{-1}$  are used. (1) is experiment and (2) is best fit.

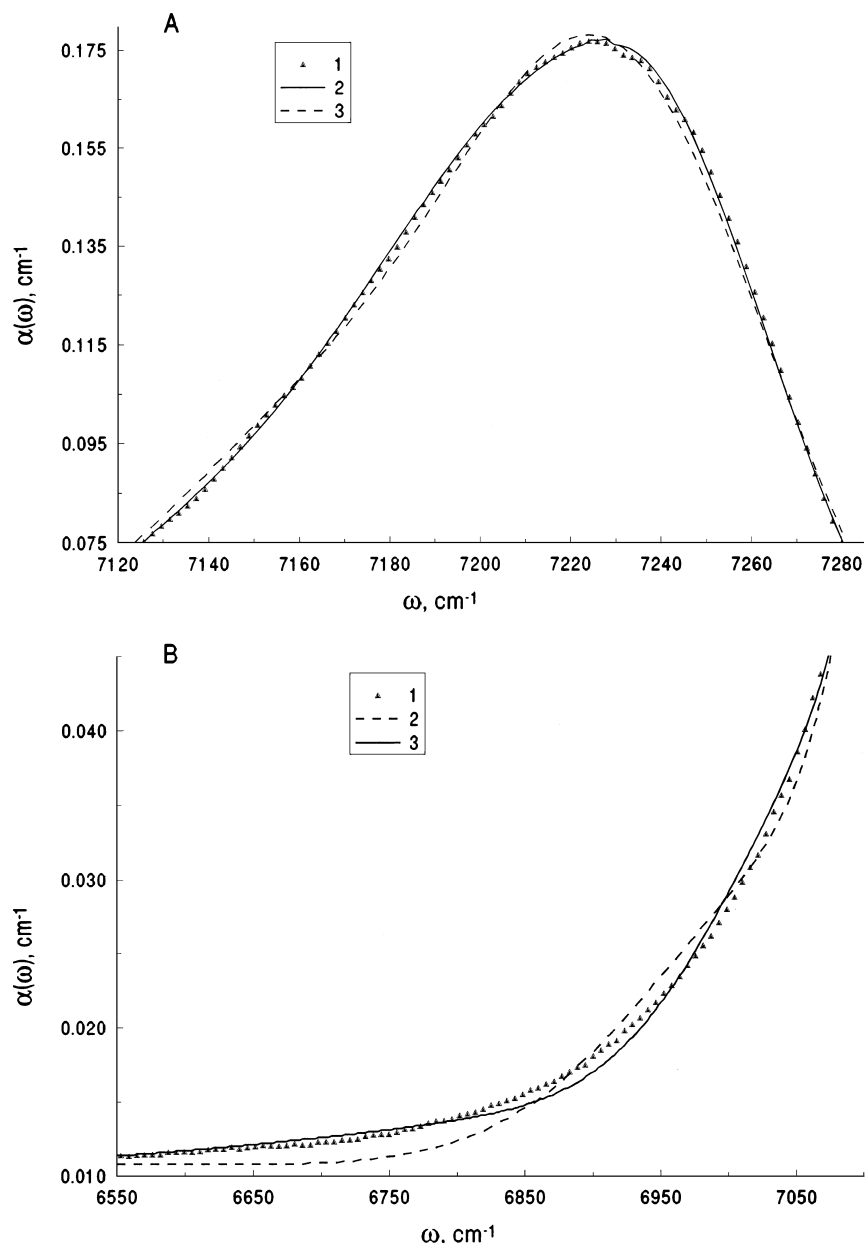
on whether the asymmetric or symmetric band contours are used. As seen from Table II, the total oscillator strength computed with Equation 2 for the 4400–4600 and 7000–7300  $\text{cm}^{-1}$  envelopes (and also for the 7300–7600  $\text{cm}^{-1}$  region lying outside the latter envelope) are in a good agreement with those calculated when simulating the envelopes with the symmetric band shapes given by Equation 1. This confirms that the band parameters found with the generalized convolution model given by Equation 2 retain a clear physical meaning.

Fig. 1 shows a quite high quality of best fit to the experimental spectrum of vitreous silica in the entire 3800–8000  $\text{cm}^{-1}$  range obtained with the asymmetric band shapes given by Equation 2. As seen from Figs 2A, 3, and 4A, the use of the asymmetric band shapes given by Equation 2 for simulating the 4400–4600 and 7000–7450  $\text{cm}^{-1}$  regions provides best fit that practically lacks systematic deviations from the experimental spectrum. On the contrary, the use of the symmetric band contours given by Equation 1 results in rather small but clearly seen systematic deviations (Figs 2B and 4). When the number of the symmetric bands under the 7000–7300  $\text{cm}^{-1}$  envelope is taken to be two (i.e., the same as that of the asymmetric bands), appreciable differences between fit and experiment occur in the 6550 to 7000  $\text{cm}^{-1}$  region (Fig. 4B). An increase in the number of the symmetric bands under the 7000–7300  $\text{cm}^{-1}$  envelope up to three (as was the case for [3–5]) improves the fit (Fig. 4B) but does not eliminate the systematic errors of the fit around the maximum of the envelope (Fig. 4A). As seen from Table II, the magnitude of the error function (3) for best fit with the asymmetric band shapes given by Equation 2 is two times less than that for the fit obtained with the greater number of the symmetric band shapes given by Equation 1. Hence it follows that the errors in the band frequencies and intensities for weak and/or greatly

overlapped bands obtainable with the dispersion analysis of the absorption spectra based on model given by Equation 2 should be appreciably less than those estimated in [9] (0.5–0.6% and 10–12%, respectively). For estimating these diminished error magnitudes, further research is necessary. In view of uncertainty in the actual error magnitudes, the band parameter values in Tables I and II are presented with the numbers of decimal figures greater than those matching the above errors from [9].

Thus, the use of the asymmetric band shapes given by Equation 2 for the 4400–4600 and 7000–7300  $\text{cm}^{-1}$  regions allows for (i) attaining the appreciably better quality of best fit to the spectrum compared to that obtainable with the symmetric band shapes given by the usual convolution model (1) and (ii) reliably deconvoluting the silica glass spectrum with the smaller number of spectral components than is the case for the symmetric band shapes. All the above indicates that (i) a certain asymmetry of the hydroxyl-related bands in the 4400–4600 and 7000–7300  $\text{cm}^{-1}$  regions of the silica glass spectrum does occur and (ii) the generalized convolution model (2) is the more accurate tool for simulating the hydroxyl-related spectra of glasses than the usual convolution model (1).

In the 4400–4600  $\text{cm}^{-1}$  region, the shape of the higher frequency absorption band (4527  $\text{cm}^{-1}$ ), judging by the  $S_{j1}/S_{j2}$  ratios (Table II column 5), is more asymmetric than that of the lower frequency band (4451  $\text{cm}^{-1}$ ). In the 7000–7300  $\text{cm}^{-1}$  region, on the contrary, the greater asymmetry occurs for the lower frequency band (7106  $\text{cm}^{-1}$ ). However, the  $\sigma_{j1}/\sigma_{j2}$  ratios (Table II column 6) indicate similar trends of variations in the asymmetry of the oscillator distribution from band to band in these regions: in each region, it is the lower frequency band that is characterized by the more asymmetric distribution. Therefore, it is possible that the



**Figure 4** Comparison of best fits to the spectrum of silica glass sample at wavenumbers greater than  $6500\text{ cm}^{-1}$  obtained with different band contours. (A) Best fits in the  $7100$  to  $7300\text{ cm}^{-1}$  region obtained when simulating the envelope with different band contours. (1) is experiment, (2) is best fit that uses two asymmetric band contours given by Equations 2 and 3 is best fit that uses three symmetric band contours given by Equation 1. (B) Best fits in the  $6550$  to  $7000\text{ cm}^{-1}$  region: effect of the number of symmetric band contours used for simulating the  $7000$ – $7300\text{ cm}^{-1}$  envelope. (1) is experiment and (2) and (3) are best fits that use two and three bands, respectively, with contours given by Equation 1.

same low-frequency component of the  $\nu(\text{Si})\text{O-H}$  vibration participates in the formation of the  $4451$  and  $7106\text{ cm}^{-1}$  bands and the same high-frequency component of the  $\nu(\text{Si})\text{O-H}$  vibration participates in the formation of the  $4527$  and  $7229\text{ cm}^{-1}$  bands. A small  $S_{j1}/S_{j2}$  ratio compared to the  $\sigma_{j1}/\sigma_{j2}$  ratio found for the  $4451\text{ cm}^{-1}$  band correlates with the greatest damping coefficient  $\gamma_j(\gamma_j/\omega_j)$  for this band being  $3.0 \times 10^{-2}$  compared to  $8.2 \times 10^{-3}$  for the  $4527\text{ cm}^{-1}$  band and  $\sim 3.5 \times 10^{-3}$  for bands in the  $7000$ – $7300\text{ cm}^{-1}$  region). Hence it follows that dissimilar variations, from band to band, in the asymmetry of the absorption band shapes observed for the  $4400$ – $4600$  and  $7000$ – $7300\text{ cm}^{-1}$  regions are due merely to differences in the effect of the damping coefficient on a particular bandwidth.

As mentioned above, two spectral components are quite enough for accurately simulating the  $7000$ – $7300$

$\text{cm}^{-1}$  envelope (Fig. 5 and Table II), which is in accord with a similar conclusion made in [11] with respect to the  $3600$ – $3700\text{ cm}^{-1}$  envelope covering the  $\nu(\text{Si})\text{O-H}$  fundamentals. This rejects the idea of four  $\nu(\text{Si})\text{O-H}$  components related to the O–H displacements in two kinds of bidentate groups first proposed in [2] and then used in [3, 4]. Therefore, there are yet no physical grounds to specify particular  $\nu(\text{Si})\text{O-H}$  components contributing to the  $7000$ – $7300$  and, hence,  $4400$ – $4600\text{ cm}^{-1}$  envelopes. The participation of the  $\nu(\text{Si})\text{O-H}$  vibration in the combination modes responsible for the  $4400$ – $4600\text{ cm}^{-1}$  envelope was confirmed [19] by burning out this envelope with excimer laser radiation. On the contrary, the band around  $5300\text{ cm}^{-1}$  could not be burnt out [19], which confirmed the assignment of this band [20] to the combination mode involving the  $\nu\text{H}_2\text{O}$  vibration.

TABLE III Assignments of the absorption bands in the 4000 to 7400  $\text{cm}^{-1}$  region of silica glass spectrum

Stone and Walrafen [3]		Humbach <i>et al.</i> [5]		Efimov <i>et al.</i> [9]		The given research	
$\omega_j$ ( $\text{cm}^{-1}$ )	Assignment	$\omega_j$ ( $\text{cm}^{-1}$ )	Assignment	$\omega_j$ ( $\text{cm}^{-1}$ )	Assignment	$\omega_j$ ( $\text{cm}^{-1}$ )	Assignment
Combination modes involving vibrations as follows							
4100	$\nu'(\text{Si})\text{O}-\text{H} + \delta\text{O}-\text{Si}-\text{O}$	–	–	4174	Certain $\nu(\text{Si})\text{O}-\text{H}$ and/or	4076	Unspecified
4450	$\nu'(\text{Si})\text{O}-\text{H} + \nu_s\text{Si}-\text{O}-\text{Si}$	–	–	4452	$\nu\text{H}_2\text{O}$ components	4451	Certain $\nu(\text{Si})\text{O}-\text{H}$
4520	$\nu''''(\text{Si})\text{O}-\text{H} + \nu_{as}\text{Si}-\text{O}-\text{Si}$	4521	$\nu(\text{Si})\text{O}-\text{H}$ + $\nu_{as}\text{Si}-\text{O}-\text{Si}$	4518	(unspecified) + some matrix vibrations	4527	components + $\nu_s\text{Si}-\text{O}-\text{Si}$ or $\nu_{as}\text{Si}-\text{O}-\text{Si}$
–	–	–	–	4720	–	4630	Unspecified
–	–	–	–	4910	–	4864	–
–	–	5280	$\nu(\text{Si})\text{O}-\text{H}$ + $2\nu_s\text{Si}-\text{O}-\text{Si}$	5260	–	5275	$\nu\text{H}_2\text{O} + 2\nu_s\text{Si}-\text{O}-\text{Si}$
–	–	–	–	6008	–	5807	Unspecified
–	–	–	–	–	–	6932	–
Overtone vibrations as follows							
7100	$2\nu''''(\text{Si})\text{O}-\text{H}$	7107	Certain $2\nu(\text{Si})\text{O}-\text{H}$	7030	Certain $2\nu(\text{Si})\text{O}-\text{H}$	7106	Certain $2\nu(\text{Si})\text{O}-\text{H}$
7220	$2\nu''(\text{Si})\text{O}-\text{H}$	7178	components	–	components	–	components
7260	$2\nu'(\text{Si})\text{O}-\text{H}$	7236	–	7308	–	7229	–
7380	$2\nu''''(\text{Si})\text{O}-\text{H} + \delta\text{Si}-\text{O}-\text{Si}$	7391	Unspecified	–	–	7384	Unspecified

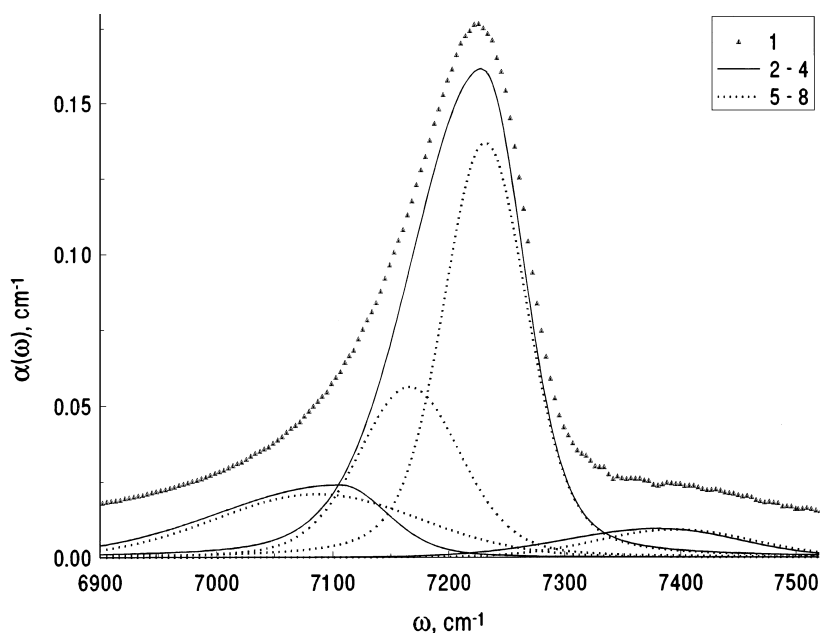


Figure 5 Individual bands deconvoluted, from the 7000 to 7450  $\text{cm}^{-1}$  region, with different band contours. (1) is experiment, (2) to (4) are the 7106, 7229, and 7384  $\text{cm}^{-1}$  bands deconvoluted using the asymmetric contours given by Equations 2, and 5 to 8 are the 7087, 7166, 7231, and  $\sim 7395$   $\text{cm}^{-1}$  bands deconvoluted using the symmetric contours given by Equation 1.

Table III compares our assignments for the absorption bands in the 4000 to 7400  $\text{cm}^{-1}$  region of silica glass spectrum that are based on the above considerations with the band assignments available in literature.

## 5. Conclusions

1. A reasonably simple analytical representation for the asymmetric band shapes in the IR absorption spectra of glasses is developed based on a certain generalization of the convolution model for the complex dielectric constant. The generalization consists in the allowance of different magnitudes of the standard deviation for an oscillator distribution that correspond to wavenumbers less and greater than the location of the distribution center. The model proposed is an appropriate tool for the

computer simulation of the asymmetric band shapes in the absorption spectra, thus being a first step to developing a general model for the complex dielectric constant of glasses that would be applicable to a broad variety of possible IR band contours.

2. A version of the dispersion analysis of the IR absorption spectra of glasses developed based on the above generalized convolution model allows for simulating the hydroxyl-related absorption maxima in the 4400–4600 and 7000–7300  $\text{cm}^{-1}$  regions of silica glass spectrum with no systematic errors throughout the contours of the maxima, thus providing the appreciably better quality of the fit than that obtainable with the available versions of the dispersion analysis based on the usual convolution model assuming the symmetric band shapes.



3. The above generalized convolution model for the complex dielectric constant requires, for adequately simulating the hydroxyl-related absorption maximum in the 7000–7300 cm<sup>-1</sup> region of silica glass spectrum, a smaller number of spectral components than is the case for the usual convolution model or, the more so, for standard deconvolution methods. Therefore, the dispersion analysis using this model is preferable from the viewpoint of avoiding the insufficiently justified incorporation of additional bands.

## References

1. P. A. VAN NIJNATTEN, J. T. BROEKHUIJSE and A. J. FABER, in Proceedings of the 5th ESG Conference "Glass Science and Technology for the 21st Century," Prague, 1999.
2. G. E. WALRAFEN and S. R. SAMANTA, *J. Chem. Phys.* **69** (1978) 493.
3. J. STONE and G. E. WALRAFEN, *ibid.* **76** (1982) 1712.
4. Y. YOKOMACHI, R. TOHMON, K. NAGASAWA and Y. OHKI, *J. Non-Cryst. Solids* **95/96** (1987) 663.
5. O. HUMBACH, H. FABIAN, U. GRZESIK, U. HAKEN and W. HEITMANN, *ibid.* **213** (1996) 19.
6. W. G. SPITZER and D. A. KLEINMAN, *Phys. Rev.* **121** (1961) 1324.
7. D. W. BERREMAN and F. D. UNTERWALD, *ibid.* **174** (1968) 791.
8. A. M. EFIMOV, "Optical Constants of Inorganic Glasses" (CRC Press, Boca Raton, USA, 1995).
9. A. M. EFIMOV, T. G. KOSTYREVA and G. A. SYCHEVA, *J. Non-Cryst. Solids* **238** (1998) 124.
10. A. M. EFIMOV, *ibid.* **253** (1999) 95.
11. *Idem.*, *Phys. Chem. Glasses* **43C** (2002) 165.
12. H. HOBERT and H. H. DUNKEN, *J. Non-Cryst. Solids* **195** (1996) 64.
13. L. A. GRIBOV, "Theory of the Infrared Spectra of Polymers" (Nauka, Leningrad, 1977).
14. YU. V. DENISOV and A. A. ZUBOVICH, *Glass Phys. Chem.* **26** (2000) 404.
15. *Idem.*, *ibid.* **25** (1999) 320.
16. G. HETHERINGTON, K. H. JACK and M. W. RAMSEY, *Phys. Chem. Glasses* **6** (1965) 6.
17. A. M. EFIMOV and P. A. VAN NIJNATTEN, *Glass Technol.* **43C** (2002) 15.
18. J. H. MALITSON, *J. Opt. Soc. Amer.* **55** (1965) 1205.
19. A. R. SILINŠ, in Proceedings of the 7th Internat. Otto Schott Colloquium, Jena, Germany, 2002.
20. L. A. SILVER and E. M. STOLPER, *J. Geol.* **93** (1985) 161.

Received 25 March 2003  
and accepted 24 February 2004